International Journal of Modern Physics C
Vol. 24, No. 6 (2013) 1350031 (8 pages)

DOI: 10.1142/S0129183113500319

GEOMETRICAL AND TRANSPORT PROPERTIES OF SEQUENTIAL ADSORPTION CLUSTERS

E. B. ARAÚJO*,§, A. A. MOREIRA*, H. J. HERRMANN*,†,
L. R. DA SILVA‡ and J. S. ANDRADE JR*

*Departamento de Física, Universidade Federal do Ceará, Campus do Pici
60451-970 Fortaleza, Ceará Brazil

†ETH Zürich, Computational Physics for Engineering Materials
Institute for Building Materials, Wolfgang-Pauli-Strasse 27
CH-8093 Zürich, Switzerland

‡Departamento de Física, Universidade Federal do Rio Grande do Norte
59072-970 Natal, Rio Grande do Norte, Brazil
§eduardo.araujo@fisica.ufc.br

Received 21 February 2013
Accepted 28 February 2013
Published 25 April 2013

We investigate transport properties of percolating clusters generated by irreversible cooperative sequential adsorption (CSA) on square lattices with Arrhenius rates given by $k_i \equiv q^{n_i}$, where n_i is the number of occupied neighbors of the site i, and q a controlling parameter. Our results show a dependence of the prefactors non q and a strong finite size effect for small values of this parameter, both impacting the size of the backbone and the global conductance of the system. These results might be pertinent to practical applications in processes involving adsorption of particles.

Keywords: Correlated percolation; cooperative sequential adsorption; transport properties; disordered media.

PACS Nos.: 64.60.ah, 72.80.Ng, 68.43.Mn, 64.60.al.

1. Introduction

Transport properties in disordered media have been successfully and extensively studied within percolation theory.[1−9] Related to percolation is random sequential adsorption (RSA) of particles on a lattice.[10] Sites are occupied sequentially independently of other sites and the system exhibits a spanning cluster at the percolation threshold.

Despite the accomplishments of the RSA model in describing disordered media,[10,11] interactions constitute an important feature in real physical systems. A common phase observed in adsorption is the $c(2 \times 2)$ (Refs. 12−14) in which

particles are arranged in a checkerboard pattern,[15] showing that nearest neighbor (NN) exclusion plays an important role in this process. This correlated filling has been studied for a chain molecule with reactive sites[16] and on square lattices, using both hierarchical rate equations[17] and percolation theory,[18] called in this case cooperative sequential adsorption (CSA). Filling of random and correlated "lattice animals" has been the subject of an extensive review.[10] The fractal dimension of the spanning cluster on CSA models has already been shown to be the same for traditional percolation.[18–20] However, the island formation process is known to be dependent on the filling ratios,[21,22] and produces clusters with peculiar shapes for different ratios. Here we show and quantify the dependence of the transport properties of the spanning cluster on different ratios.

In the CSA model, a particle irreversibly occupies an empty site i with a (multiplicative) rate given by

$$k_i \equiv q^{n_i}, \tag{1}$$

where n_i is the number of occupied NNs of site i. The parameter q controls the strength, an occupied site influences the filling of a neighboring unoccupied site: for $q > 1$ there is an attractive filling and for $q < 1$, a repulsive filling. For $q = 1$, every unoccupied site can be filled with the same probability, the model being equivalent to RSA.

2. Method

We implement this model on a square lattice of size L with periodic boundary conditions in horizontal direction. At each iteration step, we fill a random unoccupied site i chosen with probability

$$P_i = \frac{q^{n_i}}{\sum_{n_j} T_{n_j} q^{n_j}}, \tag{2}$$

where T_{n_j} is the total number of sites with n_j NN and $q \neq 0$. Figure 1 illustrates the model for several values of q. For the special case of $q = 0$, we notice that in the early stages of the process for very low q,

$$\lim_{q \to 0} T_0 P(0) = 1. \tag{3}$$

Hence, only sites with unoccupied NN would be filled and the system would never percolate. Filling would occur as in RSA with NN exclusion and stop at a jammed state with an occupation fraction of 0.365. [17,23–28] We modify the model for the special case of $q \to 0^+$, labeled henceforth $q = 0$, to obtain results compatible with this limit in the following way. Sites are filled with NN exclusion until the system reaches the jammed state. Then, all clusters in the system have size one, but no spanning cluster is formed yet. Next, sites with only one neighbor are then allowed to be occupied. When these sites are extinguished, the ones with two neighbors are then

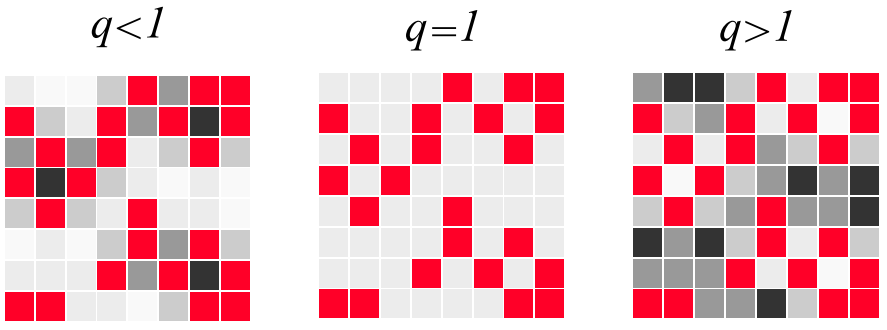

Fig. 1. (Color online) Representation of the CSA process on a square lattice for noninteracting ($q = 1$), repulsive ($q < 1$) and attractive ($q > 1$) particles with the same occupied sites (in red). Empty sites are shown in grayscale. The probability of occupying an empty site increases with its lightness. For non-interacting particles, the probability of occupying any empty site is the same, regardless the number of occupied NNs. For interacting particles it depends on the number of occupied NN. The difference between probabilities depends on the strength of the interaction, regulated by the parameter q and the configuration of the system.

occupied and so on, until a spanning cluster appears, promoting the global connection of the system.

Once the spanning cluster is obtained, the backbone and the cutting bonds are identified using the burning method.[29] To calculate the conductivity, we assume that there is a resistor of conductance g_{ij} between every pair of sites i and j of the system. The value of the conductance is

$$g_{ij} = \begin{cases} 1, & \text{if } i \wedge j \in \text{backbone;} \\ 0, & \text{otherwise.} \end{cases} \tag{4}$$

An arbitrary current is then applied between two sites ($i = 1$ and $i = N_{\text{back}}$, the number of sites in the backbone) in opposite sides of the spanning cluster and Kirchhoff's current law is imposed at each site. As a result, we obtain a set of coupled linear algebraic equations:

$$\sum_{i \neq j} M_{ij}(V_i - V_j) = \begin{cases} -1, & \text{if } i = 1; \\ 1, & \text{if } i = N_{\text{back}}; \\ 0, & \text{otherwise.} \end{cases} \tag{5}$$

where M is the Laplacian matrix of the backbone sites. M_{ij} is given by

$$M_{ij} = \begin{cases} n_i, & \text{if } i = j; \\ -1, & \text{if } i \text{ and } j \text{ are neighbors;} \\ 0, & \text{otherwise.} \end{cases} \tag{6}$$

We solve the system of Eqs. (5), for $i, j = 2, 3, \ldots, N_{\text{clus}}$ to obtain the voltages in each

resistor and therefore the global conductance of the system. For each quantity an average is obtained over at least 2000 realizations for a given value of L.

3. Results

The dependence on q of the percolation threshold[22] is calculated to high precision for system sizes up to $L = 4096$, as shown in Fig. 2. Also, typical realizations of the system at the critical point are shown for three distinct values of q. Previous studies indicate that this model belongs to the same universality class of traditional percolation.[18] Our data and analysis confirm that the fractal dimensions of the masses of the cluster, backbone, cutting bonds and of the conductivity are indeed the same as in traditional percolation.

Nevertheless, there is a clear difference in shape for the clusters obtained for different values of q.[18] For very small values of q, the cluster resembles a warped wire and presents a large number of cutting bonds. As q increases and the repelling force

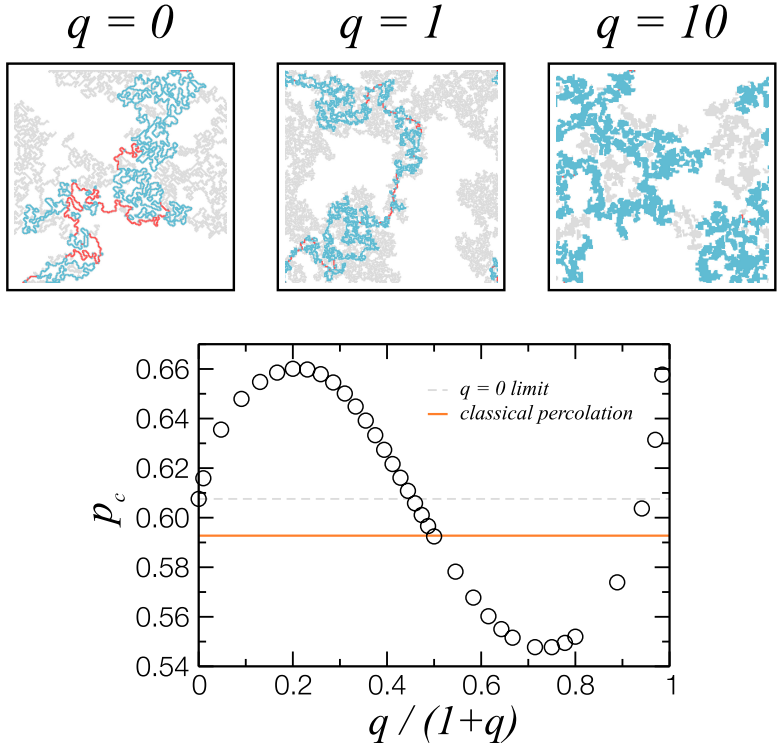

Fig. 2. (Color online) Top: typical spanning clusters on the onset of percolation for $q = 0$, $q = 1$ and $q = 10$. The spanning cluster appears in gray, the conducting backbone in blue and cutting bonds in red. For larger q, the fraction of sites of the spanning cluster present in the backbone is closer to 1. The number of cutting bonds generally decreases with q. Bottom: dependence of the percolation threshold p_c as a function of the parameter q. The orange line is the value for classical percolation, with $q/(1 + q) = 0.5$. The dashed gray line is the value for $q = 0$. Average values are obtained for $L = 4096$ and calculated over 2000 realizations.

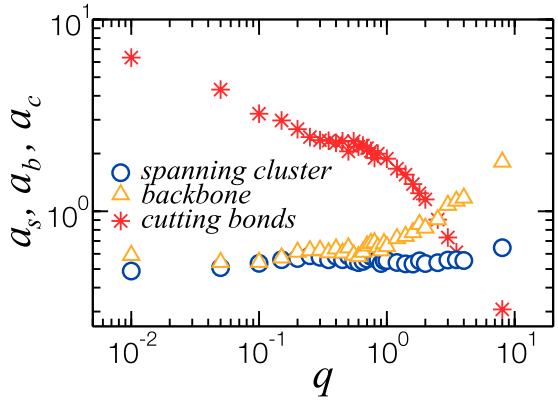

Fig. 3. (Color online) Dependence on the parameter q of the prefactor in the finite-size scaling laws for the masses of spanning cluster, $M_s = a_s L^{d_s}$, backbone, $M_b = a_b L^{d_b}$, and cutting bonds, $M_c = a_c L^{d_c}$. The cutting bonds prefactor a_c decreases monotonically with q but faster for attractive filling ($q > 1$). a_s is close to a_b for repulsive filling, but for attractive filling it increases faster.

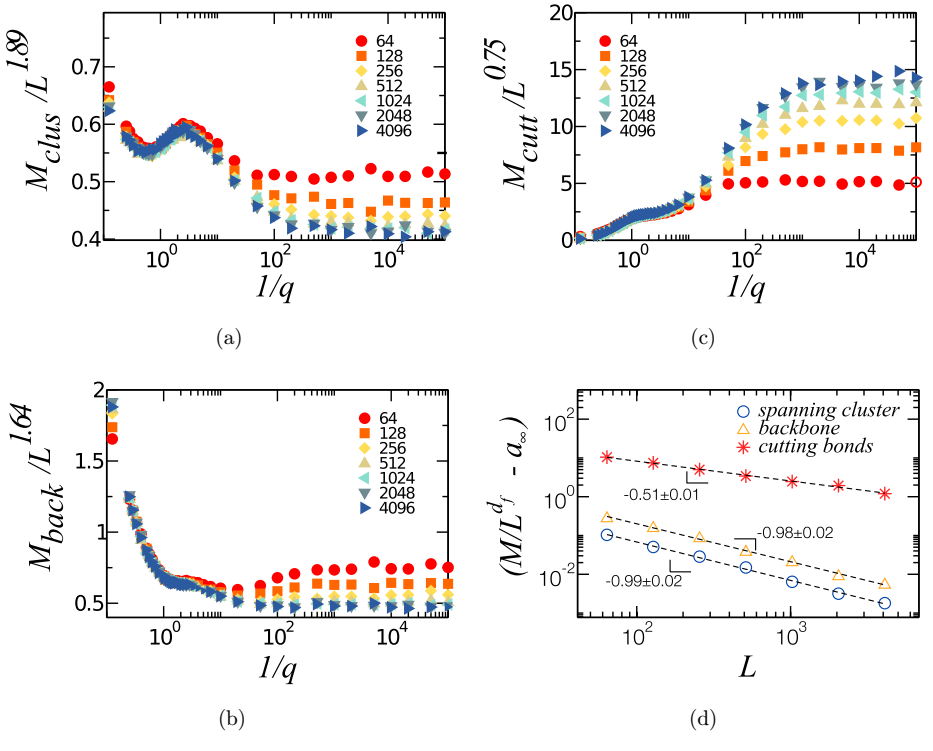

Fig. 4. (Color online) (a)−(c) Effect of the finite size of the samples on the scaling behavior of masses of the spanning cluster, backbone and cutting bonds. We show the mass divided by the system size to the power of the corresponding fractal dimension for different q. For small q, the convergence towards the thermodynamic limit becomes very slow. (d) Convergence of the a_∞ towards the thermodynamic limit for $q \to 0$. We calculated a_∞ from the best power-law fit of $(M/L^{d_f} - a_\infty)$ for each quantity.

Table 1. Values of the low q prefactor a_∞ for which the curves in Fig. 4 converge, calculated by finding the best fit of $(M/L^{d_f} - a_\infty)$ using a power-law function. The exponent of the power law, α, is also given.

Low q prefactor	a_∞	α
Spanning cluster mass	0.4104	-0.99 ± 0.02
Backbone mass	0.4708	-0.98 ± 0.02
Cutting bonds mass	15.51	-0.51 ± 0.01

becomes weaker (and turns to attraction for $q > 1$), the clusters become more massive. At the same time more sites are present in the backbone and there are less cutting bonds present.

We measure this effect calculating the prefactors from power-law fits at criticality for each mass with system size, $M_s = a_s L^{d_s}$, backbone, $M_b = a_b L^{d_b}$ and $M_c = a_c L^{d_c}$, where d_s, d_b and d_c are the corresponding critical exponents. The results are shown in Fig. 3. While the spanning cluster mass prefactor, a_s, varies little with q, the cutting bonds mass prefactor a_c decreases with q. For repulsive filling ($q < 1$) the backbone mass prefactor a_b is close to a_m but increases faster for attractive filling ($q > 1$). As a result, more sites of the spanning cluster are present in the backbone. These quantities, however, deviate from the expected power-law behavior depending on the value of q. For $q \ll 1$, there are strong finite size effects, as shown in Fig. 4. We plot the masses of the spanning cluster, backbone and cutting bonds divided by the system size to the power of their corresponding fractal dimension (the prefactor for that system size) as function of q. For small q, the convergence towards the thermodynamic limit becomes very slow. We show that the low q prefactor converges to a finite limit a_∞ as a power law of the system size. These values are shown in Table 1.

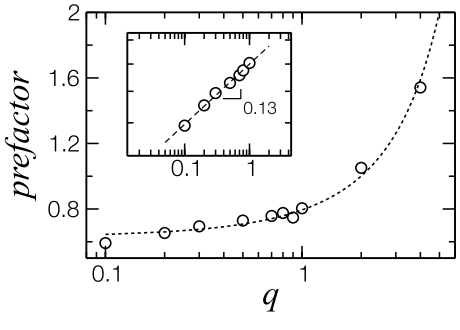

Fig. 5. Behavior of the prefactor a of the conductance as a function of q. The calculated prefactors increase monotonically with q in this range, showing that clusters formed by repulsive particles are particularly poor conductors as compared to ones formed by attractive particles. The dashed line is an exponential guide for the eyes. In the inset is shown the behavior of the prefactor as q approaches 0. The dashed line is a power law with exponent 0.13. Each point is an average over 5000 realizations. The error bars are smaller than the symbols.

The results for the prefactor of the global electrical conductance are shown in Fig. 5 for $q \in [0.1, 4]$. In this range it increases monotonically with q. For repulsive filling it increases slowly, being well fitted by a power law with exponent 0.13. For $q = 4$, the global conductance prefactor is more than 50% above the value of traditional percolation. This indicates that the more attractive the particles are, the better conductor is the conducting backbone cluster.

4. Conclusions

In summary, we have studied transport properties of percolating clusters generated by the CSA model with NNs correlations given by multiplicative rates modulated by a parameter q. Our results confirm that the mass of the backbone and the number of cutting bonds as well as the global conductance scale as power laws with the system size with the same exponents as in traditional percolation. We have shown that changes in the parameter q result in changes in all prefactors of these properties. These changes affect the spanning cluster shape, the coverage of the backbone, the number of cutting bonds and the global conductance of the system. As q becomes large, i.e. within the very attractive interaction regime, occupied sites are more likely to have occupied NN. This increases the fraction of sites in the backbone, allowing alternative paths for the current to flow in the cluster thus increasing the conductance of the system. Finally, we have shown the strong finite size effect for $q \ll 1$ and calculated the limiting values of the corresponding power-law prefactors.

Acknowledgments

We acknowledge financial support from the Brazilian agencies CNPq, CAPES, FUNCAP and European Research Council (ERC) Advanced Grant 319968-FlowCCS.

References

1. C. McGreavy, J. S. Andrade and K. Rajagopal, *Chem. Engrg. Sci.* **47**, 2751 (1992).
2. M. B. Isichenko, *Rev. Mod. Phys.* **64**, 961 (1992).
3. A. Aharony and D. Stauffer, *Introduction to Percolation Theory* (CRC Press, 1994).
4. J. S. Andrade, D. A. Street, T. Shinohara, Y. Shibusa and Y. Arai, *Phys. Rev. E* **51**, 5725 (1995).
5. J. S. Andrade, D. A. Street, Y. Shibusa, S. Havlin and H. E. Stanley, *Phys. Rev. E* **55**, 772 (1997).
6. H. E. Stanley, J. S. Andrade, S. Havlin, H. A. Makse and B. Suki, *Physica A* **266**, 5 (1999).
7. J. S. Andrade, H. J. Herrmann, A. A. Moreira and C. L. N. Oliveira, *Phys. Rev. E* **83**, 031133 (2011).
8. A. A. Moreira, C. L. N. Oliveira, A. Hansen, N. A. M. Araújo, H. J. Herrmann and J. S. Andrade, *Phys. Rev. Lett.* **109**, 255701 (2012).
9. N. Posé, N. A. M. Araújo and H. J. Herrmann, *Phys. Rev. E* **86**, 051140 (2012).
10. J. W. Evans, *Rev. Mod. Phys.* **65**, 1281 (1993).

11. A. Cadilhe, N. A. M. Araújo and V. Privman, *J. Phys. Condens. Mat.* **19**, 065124 (2007).
12. I. Jäger, *Surf. Sci.* **398**, 342 (1998).
13. S. L. Chang and P. A. Thiel, *Phys. Rev. Lett.* **59**, 1171 (1987).
14. J. W. Evans, *J. Chem. Phys.* **87**, 3038 (1987).
15. E. A. Wood, *J. Appl. Phys.* **35**, 1306 (1964).
16. J. B. Keller, *J. Chem. Phys.* **37**, 2584 (1962).
17. J. W. Evans, D. R. Burgess and D. K. Hoffman, *J. Chem. Phys.* **79**, 5011 (1983).
18. J. W. Evans and D. E. Sanders, *J. Vac. Sci. Technol. A* **6**, 726 (1988).
19. S. R. Anderson and F. Family, *Phys. Rev. A* **38**, 4198 (1988).
20. C. S. Dias, N. A. M. Araújo and A. Cadilhe, *Phys. Rev. E* **85**, 041120 (2012).
21. J. W. Evans, R. S. Nord and J. A. Rabaey, *Phys. Rev. B* **37**, 8598 (1988).
22. D. E. Sanders and J. W. Evans, *Phys. Rev. A* **38**, 4186 (1988).
23. P. Meakin, J. L. Cardy, E. Loh and D. J. Scalapino, *J. Chem. Phys.* **86**, 2380 (1987).
24. D. J. Dwyer, G. W. Simmons and R. P. Wei, *Surf. Sci.* **64**, 617 (1977).
25. J. Kertesz, B. K. Chakrabarti and J. Duarte, *J. Phys. A, Math. Gen.* **15**, L13 (1982).
26. A. Baram and D. Kutasov, *J. Phys. A, Math. Gen.* **22**, L251 (1989).
27. Y. Fan and J. K. Percus, *Phys. Rev. Lett.* **67**, 1677 (1991).
28. R. Dickman, J. S. Wang and I. Jensen, *J. Chem. Phys.* **94**, 8252 (1991).
29. H. J. Herrmann, D. C. Hong and H. E. Stanley, *J. Phys. A, Math. Gen.* **17**, L261 (1984).